ceramics

MDPI

Article

Coatings Based on Organic/Non-Organic Composites on Bioinert Ceramics by Using Biomimetic Co-Precipitation

Tomasz Engelmann [1,†], Gaëlle Desante [1,†], Norina Labude [2], Stephan Rütten [3], Rainer Telle [1], Sabine Neuss [2,4] and Karolina Schickle [1,*]

1 Department of Ceramics and Refractory Materials, RWTH Aachen University, Mauerstraße 5, 52064 Aachen, Germany; tomasz.engelmann@rwth-aachen.de (T.E.); desante@ghi.rwth-aachen.de (G.D.); telle@ghi.rwth-aachen.de (R.T.)
2 Institute of Pathology, RWTH Aachen University Hospital, Pauwelsstrasse 30, 52074 Aachen, Germany; nlabude@ukaachen.de (N.L.); sneuss-stein@ukaachen.de (S.N.)
3 Electron Microscopic Facility, RWTH Aachen University Hospital, Pauwelsstrasse 30, 52074 Aachen, Germany; sruetten@ukaachen.de
4 Helmholtz Institute for Biomedical Engineering, Biointerface Group, RWTH Aachen University Hospital, Pauwelsstrasse 30, 52074 Aachen, Germany
* Correspondence: k.schickle@ghi.rwth-aachen.de; Tel.: +49-241-80-98338; Fax: +49-241-80-82027
† Tomasz Engelmann and Gaëlle Desante contributed equally to this publication.

Received: 20 February 2019; Accepted: 1 April 2019; Published: 3 April 2019

Abstract: Bioinert ceramics have been commonly used in the field of orthopedic and dentistry due to their excellent mechanical properties, esthetic look, good biocompatibility and chemical inertness. However, an activation of its bioinert surface could bring additional advantages for better implant-integration in vivo. Therefore, we introduce an innovative biomimetic co-precipitation technique by using modified simulated body fluid (SBF) to obtain a composite coating made of organic/non-organic components. The zirconia samples were soaked in SBF containing different concentrations of protein (0.01, 0.1, 1, 10 and 100 g/l). Bovine serum albumin (BSA) was applied as a standard protein. During the soaking time, a precipitation of calcium phosphate took place on the substrate surfaces. The proteins were incorporated into the coating during precipitation. Morphology changes of precipitated hydroxyapatite (HAp) due to the presence of proteins were observed on SEM-images. The presence of proteins within the coating was proven by using SEM/energy dispersive X-ray spectroscopy (EDX) and immunohistochemical analysis. We conclude that it is possible to co-precipitate the organic/non-organic composite on inert ceramic by using the wet-chemistry method. In future studies, BSA could be replaced by targeted proteins appropriate to the application area. This method could create new biomaterials, the surfaces of which could be tailored according to the desires and requirements of their use.

Keywords: high-strength ceramics; biomimetic coating; modified simulated body fluid; co-precipitation; functionalization

1. Introduction

The functionalization of inert implant surfaces is an area of research focus since it has been proven that the crucial processes take place directly on the implant surface immediately after implantation. One of the most common methods for the bioactivation of an implant surface is calcium phosphate (CaP)-coating. CaP-coatings can be obtained by using plasma spraying, sputtering deposition, sol-gel coatings, electrochemical deposition, or biomimetic deposition [1–4]. The advantage of the latter method—biomimetic deposition—is its cold character. This process proceeds at room temperature and no thermal-post-treatment is required. This allows for new possibilities to introduce additional

thermo-sensitive biological agents during the CaP-precipitation process to design a multifunctional surface containing tailored properties according to the intended application.

Various studies present the co-precipitation of BSA proteins and CaP on metal substrates, mainly on Ti-based alloys [5–10]. Liu et al. successfully co-precipitated BSA and calcium phosphate on Ti4Al-substrates by using biomimetic precipitation [5]. The applied concentration of SBF in this study was 5×. Immunohistochemical analyses indicated that the protein content incorporated into the CaP-coating could be detectable with BSA-concentrations higher than 0.001 g/l. Interestingly, the authors could show that the higher the protein concentration, the lower the coating thickness and the lower the crystallinity of the coating. Moreover, with increased concentrations of BSA, the coating was more compact. In the follow-up study, the authors showed that the incorporation of BSA into the coating significantly improved the mechanical behavior of coatings [6], which they supported with evidence. The strong influence on the calcium phosphate precipitation and crystal formation due to the presence of organic biological agents in SBF on a sample of BSA was confirmed by further independent studies [7–9]. It was proven that without BSA addition, a mixture of octacalcium phosphate (OCP) and hydroxyapatite (HAp) was formed, while with the addition of BSA, only HAp could be detected. Areva et al. observed an influence of the addition of BSA in SBF on the concentration of 1 g/l on CaP-precipitation. BSA allowed the initiation of CaP-crystal nuclei; however, it inhibited its growth [10].

Combes and Rey focused on the mechanism of CaP-precipitation on collagen I in the presence of BSA, since in some studies an addition of BSA is described as inhibitor while in others it is described as a promotor of calcium phosphate formation [11]. The authors assumed that lower concentrations of BSA in SBF (< 10 g/l) would improve crystal growth in contrast with high concentrations (> 10 g/l) which appear as an inhibitor of CaP-crystallization. They dissociated the influence of BSA in two processes: nucleation and crystal growth. In the presence of BSA, the proteins adsorb to the crystal nucleus, and that causes the stabilization of the crystal owing to it achieving a critical nucleus size. The lower BSA concentration effects a higher nucleus amount, which accelerates the crystal growth. When the BSA concentration achieves a critical level, the adsorption of proteins is too high, and this inhibits ion diffusion from the solution into the crystals and in consequence prevents crystal growth.

The aim of the present study was to show, as a proof of principle, that it is possible to biomimetically functionalize not only metal substrates but also ceramic implants by the example of zirconia. Moreover, we presented a very wide range of different BSA concentrations in SBF to define a limit of concentration for BSA content as a promotor of CaP-crystal formation as well as growth. In this study, we also discuss the influence of the sedimentation of proteins in the solution while precipitating as an important aspect of the nucleation and crystal growth processes. Coatings obtained by the biomimetic approach are promising for implant integration with the surrounding hard tissues compared to coatings obtained using other synthetic methods. The multifunctional character of the coating could be used in future to design a tailored implant surface according to the requirements of its use.

2. Material and Methods

2.1. Simulated Body Fluid

The 2× concentrated SBF solution was prepared according to Tanahashi et al. [12]. Briefly, chemicals were added into 37 °C warmed ultra-pure water under constant stirring consecutively as follows: NaCl, $NaHCO_3$, KCl, K_2HPO_4, $MgCl_2 \cdot 6H_2O$, 1.0M HCl, $CaCl_2 \cdot 2H_2O$, Na_2SO_4, and TRIS. The 2× SBF was used each time immediately after fresh preparation.

2.2. Substrate Preparation and Functionalization

To produce specimens for the HAp-coating, commercially available press-appropriated zirconia granulates (TZ-3YS-E, Tosoh, Japan) were uniaxially pressed (p = 100 MPa) and subsequently sintered

at 1450 °C for 2 h. Such prepared samples were then ground and polished using SiC-abrasive paper and diamond paste, with a last polishing step at the 15 µm grit site. The polishing process was ended at this stage to obtain sharp edges on the substrate surface.

For the functionalization of bioinert zirconia, the wet-chemistry method was chosen. Two paths were applied to modify the ZrO_2-surface. The first one was based on the precipitation of calcium phosphate crystals on inert ceramics by using modified 2× concentrated SBF containing BSA proteins. The concentrations of BSA in SBF solution were 0.01, 0.1, 1, 10 and 100 g/l. To obtain the organic/non-organic coating, ZrO_2 samples were immersed in 6 ml of SBF/BSA solution and incubated at 40 °C for three days. The second batch was at first pre-coated with an HAp-layer by using SBF without proteins. The samples were immersed in 2× concentrated SBF (in 6 ml each) and subsequently incubated at 40 °C for three days. During the coating process, samples were placed in a vertical position to avoid the influence of the sedimentation of precipitated crystals within the solution (Figure 1). Afterwards, the samples were gently rinsed with bidistilled water and were placed into the modified SBF solutions containing BSA (the same concentrations as described above: 0.01, 0.1, 1, 10 and 100 g/l) and incubated for a further three days at 40 °C.

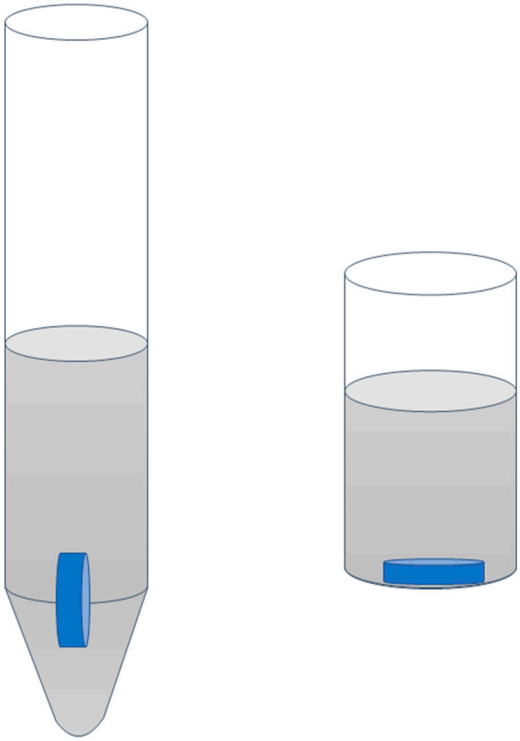

Figure 1. Experimental setting up for the co-precipitation of hydroxyapatite (HAp) and bovine serum albumin (BSA) on ZrO_2 surfaces in vertical and horizontal positions.

To evaluate the influence of the sedimentation of proteins during the precipitation process and crystal growth, all batches were divided into samples positioned i) horizontally and ii) vertically. The schematic illustration of the experimental set-up is presented in Figure 1.

2.3. Evaluation of Introduced Proteins into the HAp Coating

BSA/Alexa FluorTM 488 conjugates (Molecular Probes, Eugene, OR, USA) were applied to visualize the incorporated proteins into the surface. For this method, two concentrations of BSA in solutions of 0.1 and 0.01 g/l were chosen. To evaluate the role of the sedimentation of protein in the solution, the coating produced on horizontally and vertically positioned samples were compared. Horizontally and vertically coated samples with HAp without proteins were applied

as a control. Samples were imaged by using a fluorescence microscope (AXIO Imager M2m, Zeiss, Wetzlar, Germany).

2.4. Substrate and Coating Characterization

To determine the morphological changes on the substrate surfaces after soaking in SBF, scanning electron microscopy (Environmental Scanning Electron Microscope, ESEM XL30 FEG, FEI, Eindhoven, The Netherlands) was applied. Before microscopy, the samples were coated by using a Sputter-Coater (Sputter Coater EM SCD500, Leica, Wetzlar, Germany) with a 12.5 nm gold–palladium coating. It was possible to visualize HAp-crystals on the substrate surface. Moreover, the thickness of HAp-coatings could be measured by the imaging of the cross-section of ZrO_2-substrates. The cross-sections of the samples were prepared by embedding the samples in polymer and polishing the area of interest.

3. Results

Figure 2 shows the results of the SEM-morphology analysis of coated samples by using the wet-chemistry method, where the BSA was added to the SBF-solution directly from the beginning of the crystal precipitation process on the vertically placed samples. The control sample (BSA-0-v) as well as samples coated in SBF-solution containing 0.01 g/l BSA (BSA-0.01-v) exhibit typical coral-like crystal structures with approximately 100-nm long crystal plates (Figure 2a,b). In contrast, the morphology of crystals precipitated from the SBF containing a BSA concentration >0.1 g/l was altered. On those surfaces, the fine nano-crystalline structures can be detected on the substrate surface corresponding to crystal nuclei (Figure 2c–e). No crystal formation could be found on the samples soaked in SBF-solution containing 100 g/l BSA (Figure 2f). The crystal morphology of the horizontal samples was analogous to the structures found on the perpendicularly placed samples. However, additional crystal agglomerates exhibiting the same morphology were present on the basic coating (Figure 3).

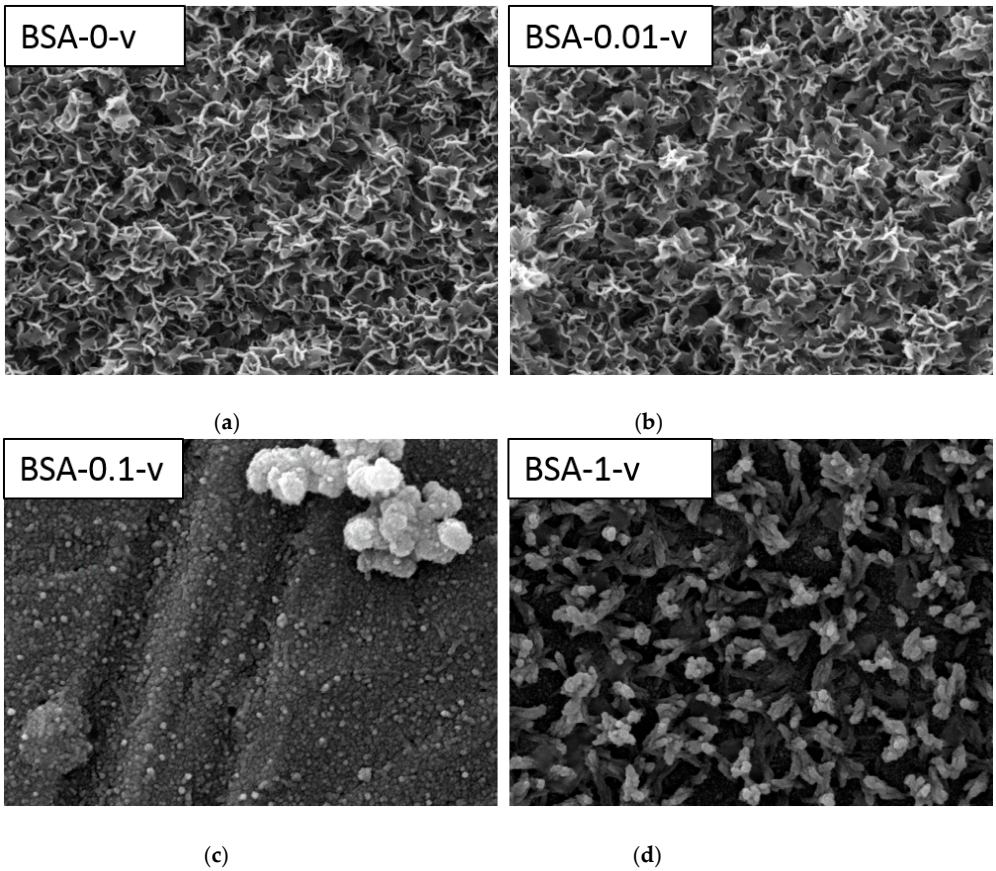

Figure 2. *Cont.*

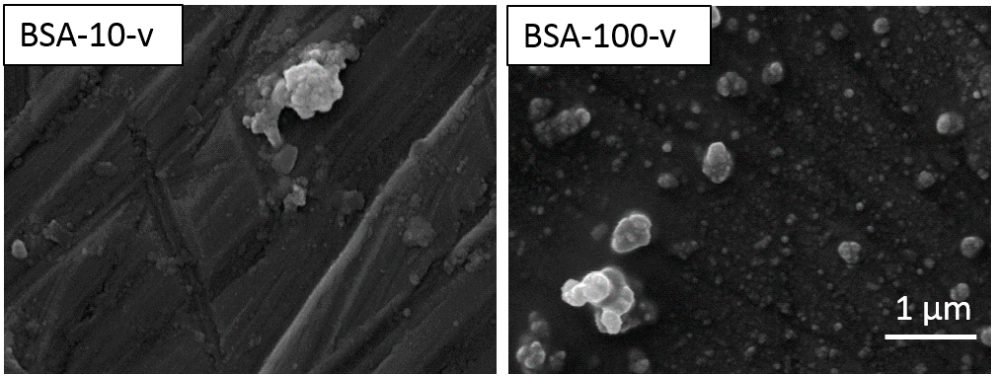

(**e**) (**f**)

Figure 2. SEM view of samples coated with HAp/BSA without pre-coating in the vertical position (BSA-0-v top left) (**a**) without BSA, (BSA-0.01-v top right) (**b**) from simulated body fluid (SBF) containing 0.01 gL^{-1} BSA, (BSA-0.1-v middle left) (**c**) from SBF containing 0.1 gL^{-1} BSA, (BSA-1-v middle right) (**d**) from SBF containing 1 gL^{-1} BSA, (BSA-10-v down left) (**e**) from SBF containing 10 gL^{-1} BSA, and (BSA-100-v down right) (**f**) from SBF containing 100 gL^{-1} BSA.

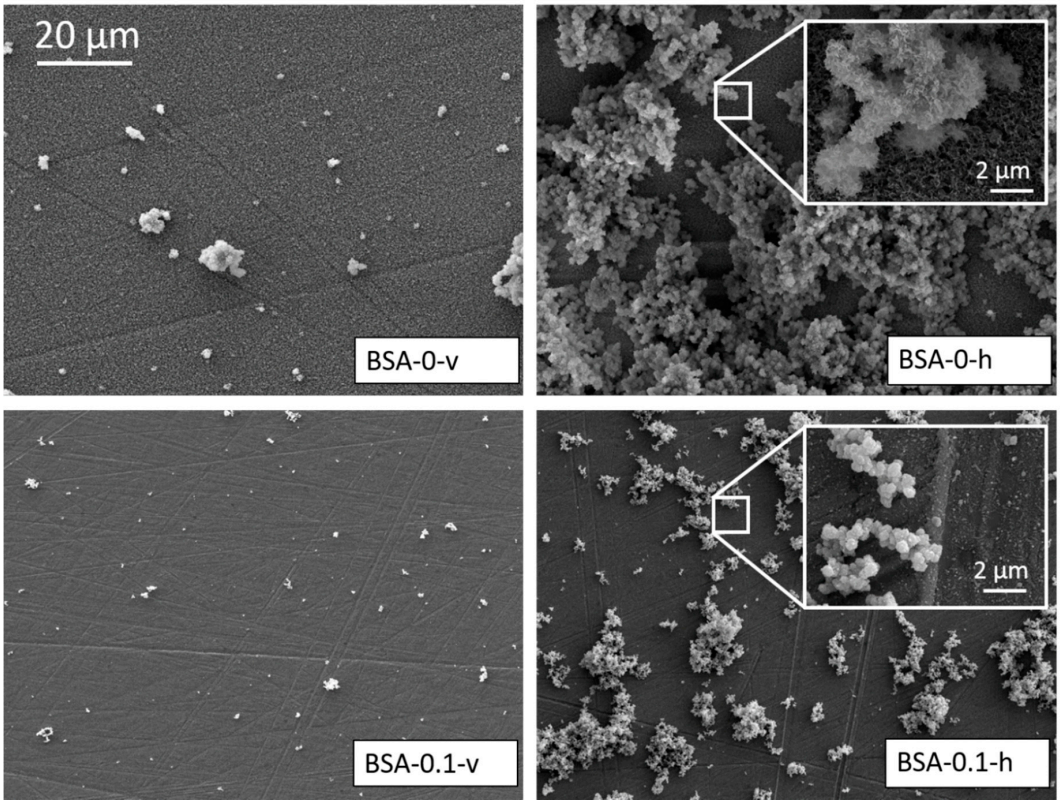

Figure 3. Comparison of horizontal (right) and vertical (left) coated samples in solution without BSA (BSA-0 top) or 0.1 gL^{-1} BSA (BSA-0.1 down). The basic coating was comparable in both cases. On the horizontal samples (on the right), additional granules precipitated within the solution and sedimented on the surface could be seen.

All pre-coated samples (HAp-BSA-0-v up to HAp-BSA-100-v) after three days soaking in different BSA concentrations in SBF exhibit the same coral-like structured coatings which are typical for HApp. However, with higher BSA concentrations, the crystal structure appears to be denser and more protein-overlaid (Figure 4).

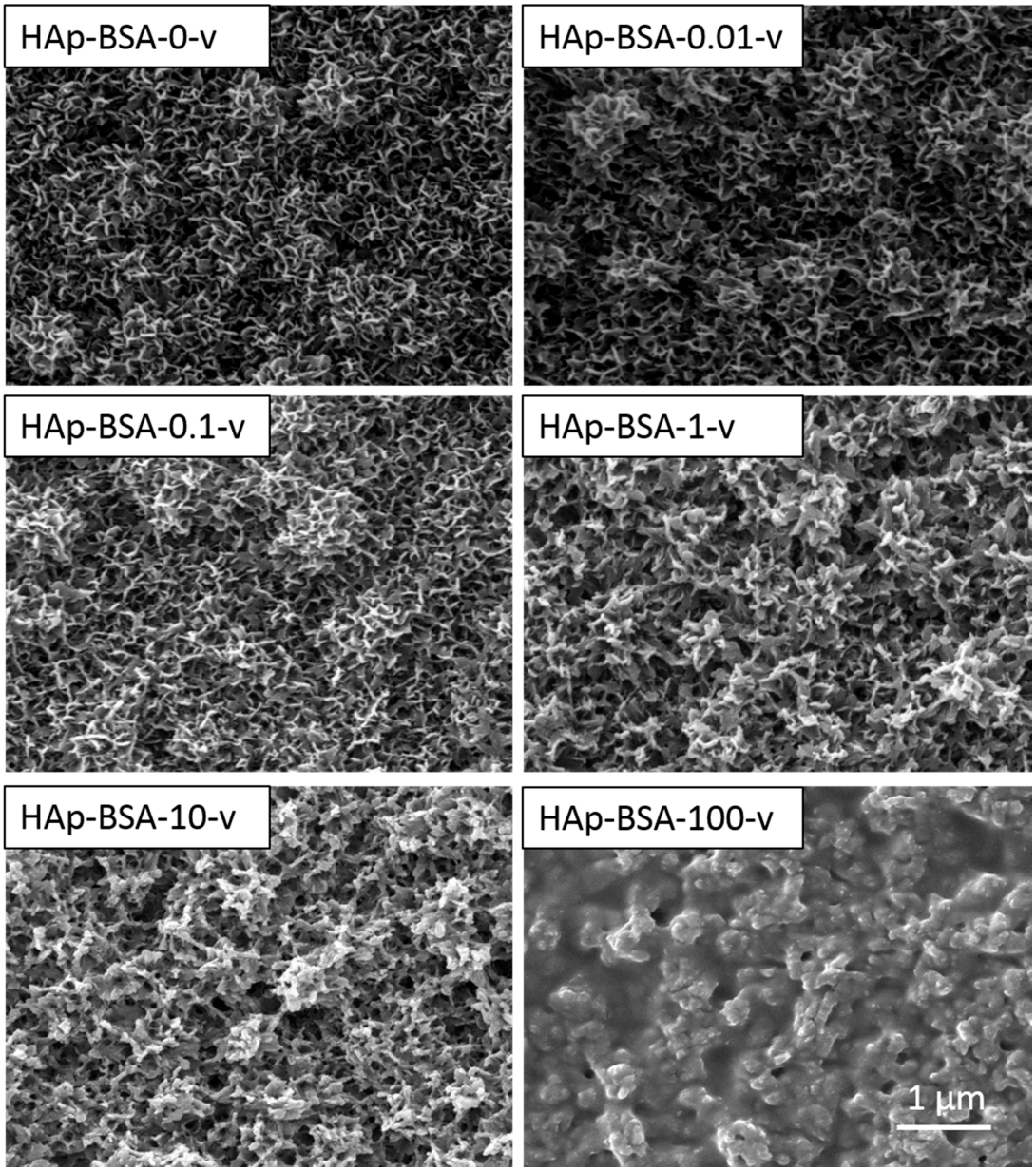

Figure 4. SEM view of samples coated with HAp/BSA with HAp pre-coating in the vertical position (HApp-BSA-0-v top left) without BSA, (HApp-BSA-0.01-v top right) from SBF containing 0.01 gL^{-1} BSA, (HApp-BSA-0.1-v middle left) from SBF containing 0.1 gL^{-1} BSA, (HApp-BSA-1-v middle right) from SBF containing 1 gL^{-1} BSA, (HApp-BSA-10-v down left) from SBF containing 10 gL^{-1} BSA, and (HApp-BSA-100-v down right) from SBF containing 100 gL^{-1} BSA.

The incorporation of proteins within the HAp-coatings was visualized by using fluorescence microscopy to detect BSA/Alexa-FluorTM-488 conjugates, which give a green signal. Figure 5 shows the results of the measurements performed for the samples prepared in a horizontal as well as vertical position for 0.1 and 0.01 g/l of conjugates in the SBF-solution (Figure 5). The intensity of the green signal is stronger with increasing protein concentration in the solution. Additionally, to quantify the amount of proteins within the coating, the carbon content on the surface was measured by using EDX (Figure 6).

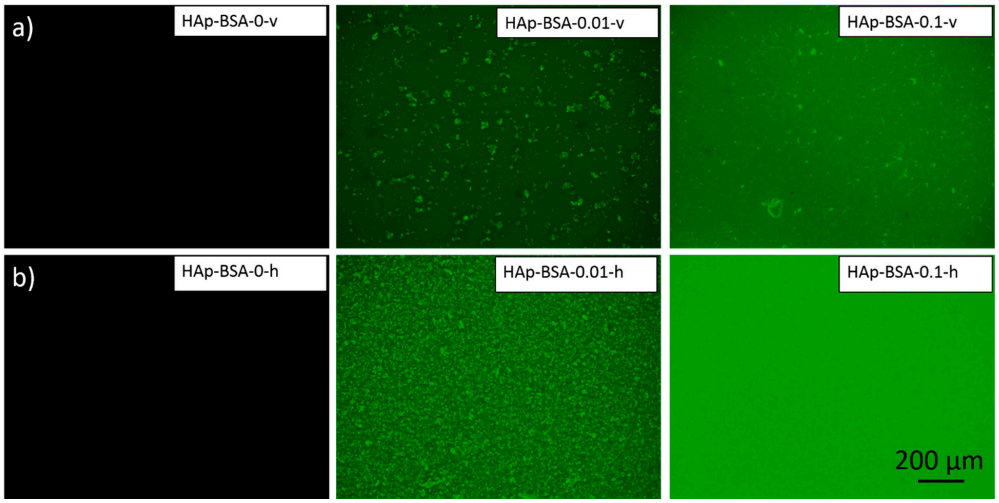

Figure 5. Fluorescence images of the vertically (**a**) and horizontally (**b**) coated samples by using precipitation from the SBF solution containing no protein, 0.01 and 0.1 gL^{-1} BSA.

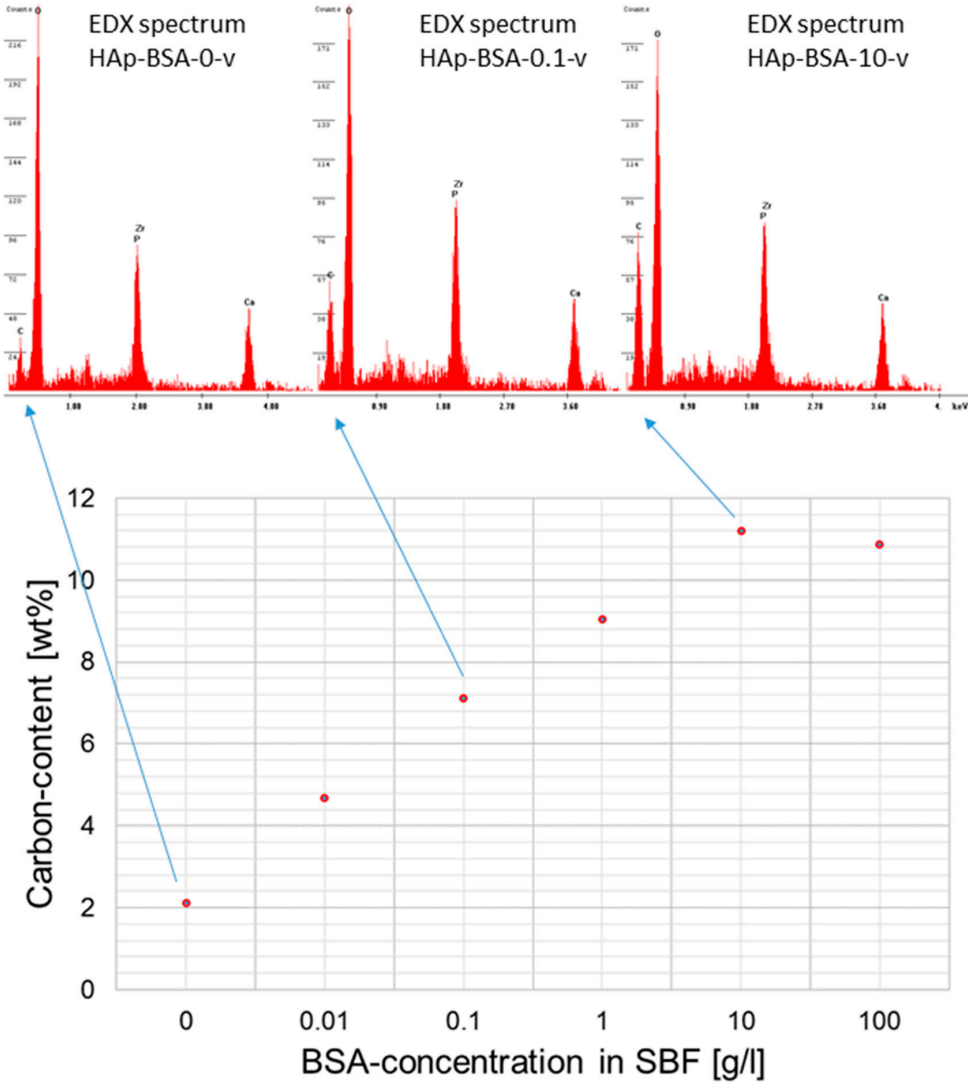

Figure 6. Top: EDX spectra from three vertically pre-coated samples. Bottom: Carbon content, which in dependent on the concentration of BSA in the solution of HAp-BSA-v samples, established by using EDX measurements.

The cross-sections of samples were imaged by using SEM to establish the influence of proteins on the thickness of the obtained coatings. Figure 7 presents the coating thickness of samples coated in the vertical position with and without HAp-pre-coating (Figure 7).

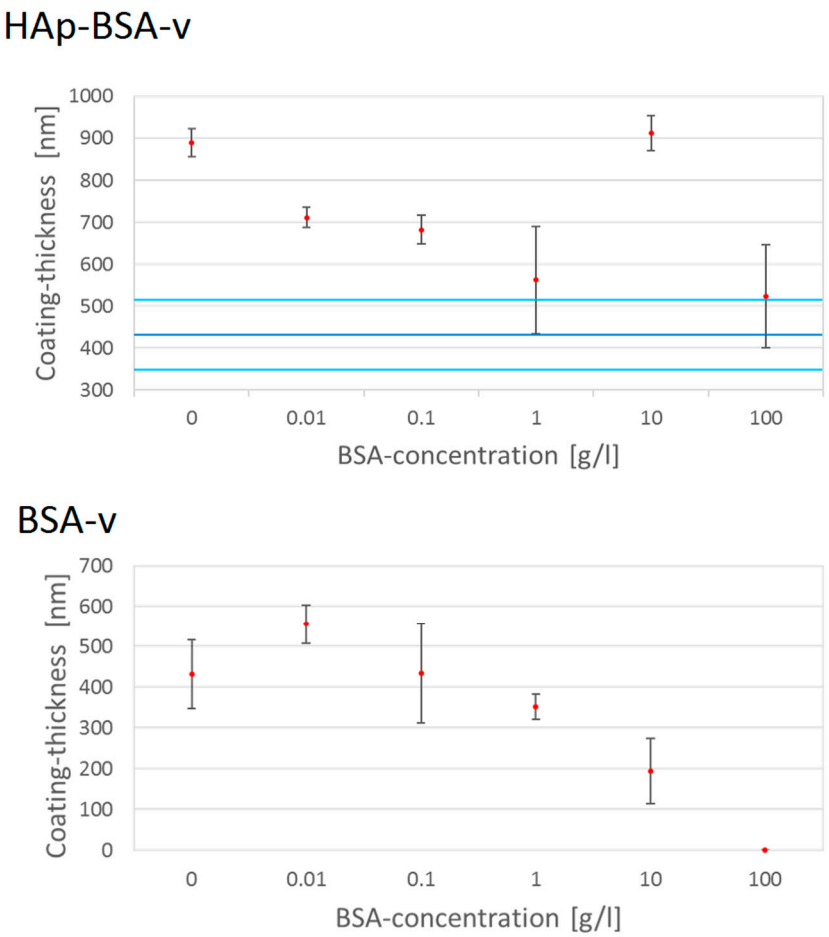

Figure 7. Coating thickness of samples treated in the vertical position with HAp (and without HAp) pre-coating.

4. Discussion

In this study, a biomimetic wet-chemistry method was applied to functionalize the inert surfaces. This method allows the introduction of the organic substances into the HAp-coating owing to the "cold character" of this process. Bovine serum albumin (BSA) was chosen as a model protein, and the influence of this biological agent on the nucleation and crystal growth of HAp on the zirconia surface was observed.

4.1. Preliminary HAp-Coatings

The SEM-analysis of samples immersed for three days in the SBF-solution presents homogenously distributed HAp-coatings on the whole substrate surface (Figure 3). The cross-section of preliminary HAp-coatings showed a thin layer with a thickness of approximately 500 nm on the vertically coated samples (BSA-0-v) and approximately 800 nm on the horizontal ones (BSA-0-h) (results not shown). On the top of the horizontally coated samples, additional HAp-agglomerates could be detected on the surface as a result of the sedimentation of precipitated HAp-crystals within the solution (Figure 3).

The morphology of the obtained coatings shows the typical HAp-structure, which is comparable with results presented elsewhere [5]. The EDX-measurements confirmed that the coating is composed of Ca and P elements. The mechanical properties of such obtained coatings play a crucial role for

their application in the medical field. Very few studies have focussed on establishing the strength and adhesion of biomimetic CaP-coatings [13–15]. Moreover, Liu et al. have shown that the mechanical properties of CaP coatings could be improved by the addition of organic biological agents such as BSA [6].

4.2. Influence of Biological Agents on Nucleation and HAp Crystal Growth

While the three-day incubation in SBF solution of the control samples (BSA-0-v and BSA-0-h) resulted in a thin HAp coating, the addition of BSA into the solution caused contrary results for samples without preliminary HAp coatings. By the addition of 0.01 gL^{-1}, a comparable coating to that for the preliminary HAp coating was observed. The BSA-0.01-v-sample showed the same crystal structure, and a similar Ca content according to EDX measurements as well as a comparable thickness to the control sample (Figure 2b). A higher BSA concentration than 0.01 gL^{-1} resulted in a logarithmic decrease of the Ca content and coating thickness (Figure 5). The morphology and crystal structures of the samples obtained by the addition of different concentrations of BSA in SBF (0.1 gL^{-1}, 1 gL^{-1} and 10 gL^{-1}) varied. It is suspected that the addition of the BSA to SBF stabilized the smaller HAp nuclei [16]. However, the HAp crystal growth is hindered because of the more difficult diffusion of ions to the BSA-loaded crystal nuclei. The obtained morphologies (Figure 2c,e) are similar to the nanocrystal structures of HAp presented by Smolen et al. [17]. Areva et al. suggested that the CaP layer formation in the presence of BSA in SBF was strongly retarded because of the continuous dissolution/reprecipitation processes [10]. Here, the initially formed amorphous CaP phase(s) recrystallizes into more thermodynamically stable phase(s). Radin and Ducheyne showed that the presence of BSA retards the surface reactions of non-apatite calcium phosphate, but not in the case of non-stoichiometric hydroxyapatite [18]. Wang et al. confirmed, through theoretical analysis, the correlation between the influence of the protein concentration on nucleation and the negative influence on the diffusion-controlled crystal growth as a consequence of the viscosity increase [19], as suggested previously by Combes and Rey [11]. However, the influence of the amorphous calcium phosphate phase for the process of nucleation and crystal growth is not very well understood and could also play a crucial role in the interaction with biological agents. Samples obtained by the addition of 100 gL^{-1} BSA into the SBF (BSA-100-v) did not show any CaP-growth on the surface (Figure 2f). Here, the deciding issue could be the influence of the proteins on the saturation point of the solution. It was described that the presence of BSA at a concentration of 50 gL^{-1} reduced the amount of free Ca^{2+}- and PO_4^{3-} ions, even to 44–46%. Moreover, the correlation between BSA concentration and the saturation point of the solution was observable within the whole range of the tested concentrations of BSA (0.1 gL^{-1} bis 50 gL^{-1}). It can thus be concluded that, in this work, the BSA concentration of 100 gL^{-1} triggered at least the same or even a higher reduction of the saturation point of the solution. The lower protein concentrations (0.01 gL^{-1}) showed no negative influence on the nucleation of HAp on the ZrO_2-surfaces. In contrast, the higher concentrations in SBF ($\geq$ 0.1 gL^{-1}) showed a tendency to inhibit the process of crystal growth, while the apatite-nuclei precipitation was completely inhibited by a BSA concentration of 100 gL^{-1} (Figure 2).

4.3. Influence of Biological Agents on Nucleation and CaP Crystal Growth on Pre-Coated Substrates

An analysis of the thickness of the obtained coating on CaP-precoated samples showed apatite growth for all tested samples (Figure 7) in comparison to the pre-coated control sample (BSA-0-v). However, it is visible that the thickness of the coating decreases with the increase of protein concentration in the solution. The results are in correlation with the SEM (Figure 4). The HAp-crystals obtained by lower concentrations of proteins are similar to the control sample; their morphology is sharp and their density is higher. In contrast, the coatings precipitated from the solution containing higher concentrations of BSA appear to be less crystalline and encased with proteins. The protein adhesion on the nuclei influences the ion-diffusion and transport and thus inhibits the crystal growth, as stated by Combes and Rey as well as Wang et al. [11,19].

4.4. Protein Integration within the HAp Coating

To establish the presence of proteins within the HAp coating, the BSA/Alexa Fluor TM 488 conjugate was applied instead of regular BSA in the SBF solution to co-precipitate already autofluorescence-stained proteins. The fluorescence microscope image concentration reliably showed green signals on each BSA/Alexa Fluor TM 488 conjugate-treated sample (Figure 4). The control samples (only HAp-coating) showed no fluorescence signal. The influence of the sedimentation process on the intensity of fluorescence signals proportional to the amount of proteins in the coating could also be observed. The samples coated in the horizontal position (HAp-BSA-0.01-h and HAp-BSA-0.1-h) exhibited much stronger fluorescence signals than the samples prepared in the vertical position (HAp-BSA-0.01-v and HAp-BSA-0.1-v). The results were in correlation with the chemical analysis of the coated surfaces. The content of carbon was measured: the results showed a logarithmic growth of carbon content in HAp coatings with a higher BSA concentration in SBF solution by the precipitation process (Figure 6).

5. Conclusions

In the present study, we demonstrate that higher concentrations of BSA in the SBF solution resulted in inhibiting the crystal growth and at the same time promoting the precipitation of nuclei. The results are in correlation with the theoretical consideration reported in the literature. It could be shown that it is possible to co-precipitate the organic/non-organic coatings based on HAp and BSA on ceramic surfaces. Moreover, an appropriate concentration was established to enhance crystal growth on the ZrO_2 surfaces. In future studies, this technique could be used to introduce other active, application-oriented proteins such as bone morphogenetic protein (BMP), arginylglycylaspartic acid (RGD) or hepatocyte growth factor (HGF) into the HAp coatings and improve, for example, bone growth and osseointegration or to obtain additional biofunctions.

Author Contributions: Conceptualization, G.D. and K.S.; data curation, T.E.; formal analysis, K.S.; funding acquisition, R.T., S.N. and K.S.; investigation, T.E., G.D., N.L. and S.R.; methodology, T.E. and G.D.; project administration, K.S.; supervision, G.D. and K.S.; writing—original draft, T.E. and K.S.; writing—review & editing, N.L., S.R., R.T. and S.N.

Funding: This research was funded by the Excellence Initiative of the German federal and state governments, grant number OPSF408.

Conflicts of Interest: The authors declare no conflict of interest.

References

1. Yang, Y.; Kim, K.H.; Ong, J.L. A review on calcium phosphate coatings produced using a sputtering process—An alternative to plasma spraying. *Biomaterials* **2005**, *26*, 327–337. [CrossRef] [PubMed]
2. Asri, R.I.M.; Harun, W.S.W.; Hassan, M.A.; Ghani, S.A.C.; Buyong, Z. A review of hydroxyapatite-based coating techniques: Sol–gel and electrochemical depositions on biocompatible metals. *J. Mech. Behav. Biomed. Mater.* **2016**, *57*, 95–108. [CrossRef] [PubMed]
3. Yeung, W.K.; Reilly, G.C.; Matthews, A.; Yerokhin, A. In vitro biological response of plasma electrolytically oxidized and plasma-sprayed hydroxyapatite coatings on Ti–6Al–4V alloy. *J. Biomed. Mater. Res. B Appl. Biomater.* **2013**, *101*, 939–949. [CrossRef] [PubMed]
4. Surmenev, R.A. A review of plasma-assisted methods for calcium phosphate-based coatings fabrication. *Surf. Coat. Technol.* **2012**, *206*, 2035–2056. [CrossRef]
5. Liu, Y.; Layrolle, P.; de Bruijn, J.D.; van Blitterswijk, C.; de Groot, K. Biomimetic coprecipitation of calcium phosphate and bovine serum albumin on titanium alloy. *J. Biomed. Mater. Res.* **2001**, *57*, 327–335. [CrossRef]
6. Liu, Y.; Hunziker, E.B.; Randall, N.X.; de Groot, K.; Layrolle, P. Proteins incorporated into biomimetically prepared coatings modulate their mechanical strength and dissolution rate. *Biomaterials* **2003**, *24*, 65–70. [CrossRef]
7. Wen, H.B.; de Wijn, J.R.; van Blitterswijk, C.A.; de Groot, K. Incorporation of bovine serum albumine in calcium phosphate coating on titanium. *J. Biomed. Mater. Res.* **1999**, *46*, 245–252. [CrossRef]

8. Feng, B.; Chen, J.; Zhang, X. Interaction of calcium phosphate in apatite with serum albumin. *Biomaterials* **2002**, *23*, 2499–2507. [CrossRef]
9. Kapoor, R.; Sistla, P.G.; Kumar, J.M.; Raj, T.A.; Srinivas, G.; Chakraborty, J.; Sinha, M.K.; Basu, D.; Pande, G. Comparative assessment of structural and biological properties of biomimetically coated hydroxyapatite on alumina (a- Al_2O_3) and titanium (Ti-6Al-4V) alloy substrates. *J. Biomed. Mater. Res.* **2010**, *94*, 913–926. [CrossRef] [PubMed]
10. Areva, S.; Peltola, T.; Säilynoja, E.; Laajalehto, K.; Lindén, M.; Rosenholm, J.B. Effect of albumin and fibrinogen on calcium phospate formation on sol-gel-derived titania coatings in vitro. *Chem. Mater.* **2002**, *14*, 1614–1621. [CrossRef]
11. Combes, C.; Rey, C. Adsorption of proteins and calcium phosphate materials bioactivity. *Biomaterials* **2002**, *23*, 2817–2823. [CrossRef]
12. Tanahashi, M.; Yao, T.; Kokubo, T.; Minoda, M.; Miyamoto, T.; Nakamura, T.; Yamamuro, T. Apatite coating on organic polymers by a biomimetic process. *J. Amer. Ceram. Soc.* **1994**, *77*, 2805–2808. [CrossRef]
13. Barnes, B.; Johnson, S.; Snell, R.; Best, S. Using scratch testing to measure the adhesion strength of calcium phosphate coatings applied to poly(carbonate urethane) substrates. *J. Mech. Behav. Biomed. Mater.* **2012**, *6*, 128–138. [CrossRef] [PubMed]
14. Barrere, F.; van Blitterswijk, C.A.; de Groot, K.; Layrolle, P. Influence of ionic strength and carbonate on the Ca-P coating formation from SBFx5 solution. *Biomaterials* **2002**, *23*, 1921–1930. [CrossRef]
15. Juhasz, J.A.; Best, S.M.; Kawashita, M.; Miyata, N.; Kokubo, T.; Nakamura, T.; Bonfield, W. Bonding strength of the apatite layer formed on glass- ceramic apatite-wollastonite–polyethylene composites. *J. Biomed. Mater. Res.* **2003**, *67*, 952–959. [CrossRef] [PubMed]
16. Takeuchi, A.; Ohtsuki, C.; Miyazaki, T.; Kamitakahara, M.; Ogata, S.I.; Yamazaki, M.; Tanihara, M. Heterogeneous nucleation of hydroxyapatite on protein: structural effect of silk sericin. *J. R. Soc. Interface* **2005**, *2*, 373–378. [CrossRef] [PubMed]
17. Smolen, D.; Chudoba, T.; Malka, I.; Kedzierska, A.; Lojkowski, W.; Swieszkowski, W.; Kurzydlowski, K.J.; Kolodziejczyk-Mierzynska, M.; Lewandowska-Szumiel, M. Highly biocompatible, nanocrystalline hydroxyapatite synthsized in a olvothermal process driven by high energy density microwave radiation. *Int. J. Nanomed.* **2013**, *8*, 653–668. [CrossRef] [PubMed]
18. Radin, S.; Ducheyne, P. Effect of serum proteins on solution-induced surface transformations of bioactive ceramics. *J. Biomed. Mater. Res.* **1996**, *30*, 273–279. [CrossRef]
19. Wang, K.; Leng, Y.; Lu, X.; Ren, F.; Ge, X.; Ding, Y. Theoretical analysis of protein effects on calcium phosphate precipitation in simulated body fluid. *Cryst. Eng. Comm.* **2012**, *14*, 5870–5878. [CrossRef]